Res Chem Intermed (2016) 42:5237–5252
DOI 10.1007/s11164-015-2355-0

Molecular mechanism of propane oxidative dehydrogenation on surface oxygen radical sites of VO_x/TiO_2 catalysts

Vasilii I. Avdeev[1] · Alexander F. Bedilo[1,2]

Received: 4 October 2015 / Accepted: 30 October 2015 / Published online: 25 November 2015

Abstract Minimum energy pathways of propane oxidative dehydrogenation to propene and propanol on supported vanadium oxide catalyst VO_x/TiO_2 were studied by periodic discrete Fourier transform (DFT) using a surface oxygen radical as the active site. The propene formation pathway was shown to consist of two consecutive hydrogen abstraction steps. The first step includes C_β–H bond activation of propane followed by the formation of a surface hydroxyl group V–O_tH and a propyl radical n-C_3H_7. This step with the activation energy $E^* = 0.56$ eV (54.1 kJ/mol) appears to be rate-determining. The second step involves the reaction of the bridging O_b oxygen atom with the methylene C–H bond of propyl radical n-C_3H_7 followed by the formation of a hydroxylated surface site HO_t–V^{4+}–O_bH and propene. The initial steps of the C–H bond activation during propane conversion to propanol and propene by ODH on V^{5+}–$(O_tO_b)^-$ active sites are identical. The obtained results demonstrate that participation of surface oxygen radicals as the active sites of propane ODH makes it possible to explain relatively low activation energies observed for this reaction on the most active catalysts. The presence of very active radical species in low concentration seems to be the key factor for obtaining high selectivity.

Keywords VO_x/TiO_2 catalyst · Oxidative dehydrogenation · Oxygen radicals · Propane · Reaction path

Electronic supplementary material The online version of this article (doi:10.1007/s11164-015-2355-0) contains supplementary material, which is available to authorized users.

✉ Alexander F. Bedilo
abedilo@bk.ru

[1] Boreskov Institute of Catalysis SB RAS, Prospekt Lavrentieva 5, Novosibirsk 630090, Russia

[2] Novosibirsk Institute of Technology, Moscow State University of Design and Technology Branch, Krasny Prospekt 35, Novosibirsk 630099, Russia

Introduction

Oxidative dehydrogenation (ODH) of light alkanes over transition metal oxides MO_x is of great interest for synthesis of light olefins as a practicable alternative to non-oxidative dehydrogenation. It is energetically favorable due to lower reaction temperatures and has improved catalyst lifetime due to the lack of coke deposition. Also, it is exothermic and is not limited by equilibrium. Unfortunately, non-selective combustion limits the alkene selectivity, particularly at high conversions.

During the last two decades, many metal oxide systems have been studied in oxidative dehydrogenation of light alkanes. The results obtained for ODH of light alkanes have been summarized in several good reviews [1–4]. These studies demonstrate that supported vanadia catalysts are among the most promising materials for this reaction [5–7]. Vanadia supported on different oxide supports was also shown to be a promising catalyst for various other redox processes, such as oxidation of methane, butane, ethanol, etc. [8, 9], as well as in destructive sorption of halogenated compounds [10, 11]. The activity and selectivity of such catalysts was found to depend on the local composition and structure of vanadium-containing species present at the catalyst surface. However, despite many experimental studies [8, 12, 13] and theoretical simulations [14–21] the nature of the active and selective surface sites in supported vanadia catalysts is still not well understood.

Different data suggest that either vanadyl or bridging oxygen atoms could be the active species [22]. The catalytic activity substantially depends on the used support, $V–TiO_2$ catalysts being the most active. Generally, more reducible supports give more active catalysts, although their selectivity may be not as good [4]. This result is currently not understood within the existing models. Furthermore, there is reasonable doubt that traditional diamagnetic V^{5+} species can account for the observed reactivity. In our opinion, development of new efficient catalytic systems that would allow for effective propene production with high selectivity at higher propane conversions is hardly possible without better understanding the nature of the catalytically active sites and detailed analysis of the molecular mechanism.

Propene ODH over VO_x/TiO_2 catalysts is characterized by low activation energies. Dinse et al. [23] found that the catalytic activity of vanadia supported on different oxides decreased in the following order: $VO_x/TiO_2 \approx VO_x/ZrO_2 > VO_x/CeO_2 \gg VO_x/Al_2O_3 \gg VO_x/SiO_2$. The lowest activation energy among these systems 56 ± 5 kJ/mol was reported for VO_x/TiO_2. Higher activation energies were reported for other oxides (as high as 146 ± 6 kJ/mol for VO_x/SiO_2). Shee et al. [24] reported activation energies varying from 65 to 73 kJ/mol for propane ODH over VO_x/TiO_2 with different vanadium concentrations. Activation energies from 69 to 81 kJ/mol were reported by Singh et al. [25] for propane over a series of VO_x/TiO_2 modified with phosphorous. The results of several studies were summarized in a review by Grabowski [3]. The values reported for VO_x/TiO_2 included in the review varied from 25 to 81 kJ/mol. Carrero et al. [4] recently published an excellent review summarizing the performance of vanadia catalysts on different oxide supports in propane ODH. According to their data, apparent activation for this

reaction over various VO_x/TiO_2 catalysts is 60 ± 12 kJ/mol and does not depend on the vanadium concentration.

Despite this low activation energy, propane ODH on VO_x/TiO_2 catalysts typically takes place at 450 °C or higher temperatures. The occurrence of a reaction with low activation energy at such high temperatures means that the pre-exponential factor in the reaction rate equation must be quite low. In our opinion, this clearly indicates that the reaction starts on few very active sites rather than on abundant vanadium species present in high concentration.

In our research, we pay particular attention to very active surface sites, such as electron-donor [26, 27], electron-acceptor sites [27–29], and oxygen radical species [30, 31]. Oxygen radicals have been documented over a variety of metal oxides [31–33]. These species are very reactive and can abstract hydrogen atoms from saturated hydrocarbons. It was suggested that O^- radicals were responsible for oxidative dimerization of methane at elevated temperatures [34]. Among supported vanadia catalysts, O^- radicals are readily observed by EPR during reoxidation of reduced VO_x/SiO_2 catalysts [35–38]. The formation of a V^{5+}–O^- radical anion on the surface of reduced $V^{4+}O_x$/MCM-41 catalyst after contact with gas-phase O_2 has been suggested based on the EPR data [37].

Meanwhile, monomeric and polymeric vanadium species on VO_x/TiO_2 catalysts yield no EPR signals attributable to the oxygen radicals. Still, it is possible that such EPR-silent oxygen radicals can be formed on the surface of VO_x/TiO_2 samples, at least as transient species. Recently, VO_3 clusters bound to rutile TiO_2 surface were experimentally observed under high-vacuum conditions and claimed to be the only surface vanadium species active in oxidative dehydrogenation of methanol to formaldehyde [39].

Simulation of active vanadium sites on the TiO_2 surface has been a subject of several of our recent publications [40–43]. In particular, we have recently shown by DFT calculations that oxygen isotopic exchange on supported vanadia might start on surface oxygen radicals [43]. These results suggest that these oxygen radicals may be present on the surface of oxidation catalysts under catalytic conditions. However, until now the mechanism of propane ODH over oxygen radicals on the surface of VO_x/TiO_2 catalysts has never been studied by modern periodic DFT methods.

The main objective of this paper is to analyze the possible role of the oxygen radicals in a practically important reaction—oxidative dehydrogenation of propane to propene on supported vanadium oxide catalyst VO_x/TiO_2. As in our previous study [43], oxygen radical sites V^{5+}–$(O_tO_b)^-$ containing terminal O_t and bridging O_b oxygen atoms were constructed on the experimentally observed reconstructed anatase surface TiO_2 (001)-(4 × 1).

In this paper we demonstrate that the C_β–H bond activation in propane followed by the formation a surface hydroxyl group V–O_tH and a propyl radical with the activation energy $E^* = 0.56$ eV (54.1 kJ/mol) is the rate-determining step of propane ODH over the oxygen radical site. The obtained results prove that participation of surface oxygen radicals as the active sites of propane ODH makes it possible to explain relatively low activation energies observed for this reaction on the most active catalysts.

Models and computational details

Model of active sites for anatase-supported vanadium oxide

The structure of VO_x species on the surface of VO_x/TiO_2 catalyst with distinct oxygen-radical character on experimentally observed (1 × 4)-reconstructed anatase-TiO_2 (001) surface [44, 45] was built by isomorphic replacement of the top Ti atoms by V ones followed by reoxidation of the reduced surface V^{4+} site by an oxygen atom. Details on the construction of this surface have been presented in our earlier publications [41–43].

The resulting model of VO_x/TiO_2 surface and the projected density of states (PDOS) for it are shown in Fig. 1. The supercell included three Ti–O layers and the top VO_x layer. The atomic positions of the upper layers were obtained by the structure optimization. The experimental anatase TiO_2 lattice parameters were used for the frozen bottom Ti–O layer: $a = b = 3.78$ Å, $c = 9.51$ Å. The $[VO_x/TiO_2]$ unit is translated with a period $d = 3.78$ Å along the [100] direction and with $d = 15.12$ Å along the [010] direction. As a result, a chain of the surface VO_x species is formed along the [100] direction. As shown in Fig. 1a, the local structure of VO_x species corresponds to tetrahedral VO_4 units, which are embedded into the reconstructed TiO_2 (001) surface by two interface V–O–Ti bonds. The surface $[O_t–V–O_b]$ species includes a terminal oxygen atom, O_t , and a bridging one, O_b. The distance between the neighboring $[VO_4]$ units along the [100] direction, $d = 2.09$ Å, substantially exceeds the length of the covalent bonds $V–O_t = 1.64$ Å and $V–O_b = 1.70$ Å. This structural feature demonstrates that direct interaction of the neighboring surface units VO_4 is weak. As a result, the VO_4 units on the reconstructed TiO_2 (001) surface behave as surface species isolated from each other.

Possible formation of isolated surface species VO_x on V_2O_5/TiO_2 catalysts was analyzed by Choo et al. [46]. Using Raman and IR spectroscopy, the authors concluded that an increase in the number of hydroxyl groups on the TiO_2 support enhanced the formation of more segregated VO_x species instead of polymeric

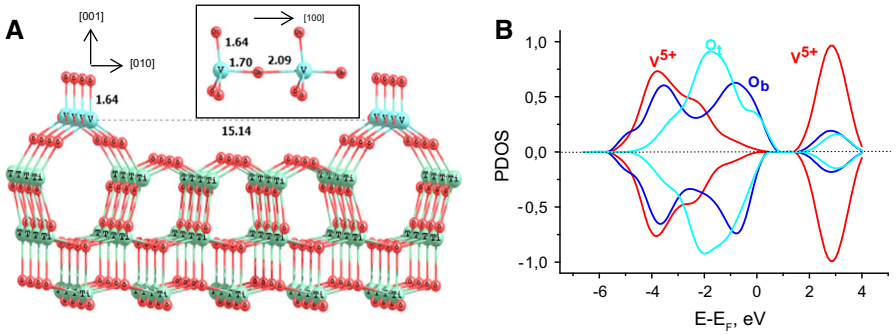

Fig. 1 **a** Model of the $[VO_4]$ active sites on the (1 × 4)-reconstructed anatase-TiO_2 (001) surface. The *inset* structure shows mutual orientation of the terminal O_t and bridging O_b oxygen atoms along the [100] direction. **b** Corresponding PDOS of the surface $[O_t–V^{5+}–O_b]$ species. The *curves above* and *below* PDOS = 0.0 show the spin-up and spin-down states, respectively. The Fermi energy E_F was taken as the reference one

chains. A similar conclusion was maid by Lapina et al. [47]. Based on the data obtained by NMR, EPR, and magnetic susceptibility, it was suggested that all surface vanadium species VO_x on V_2O_5/TiO_2 catalysts are isolated from each other. The role of isolated vanadium species [VO_4] with tetrahedral coordination in selective oxidation of light alkanes was analyzed in detail by Albonetti et al. [48].

The model suggested by us (Fig. 1a) fully meets the isolation criterion. A unique feature of isolated VO_4 active sites is the high lability of [O_t–V–O_b] species. Another important property of these sites is the radical type of the terminal O_t and bridging O_b oxygen atoms. Figure 1b demonstrates the density of states for the surface O_t–[V]–O_b species projected on the O_t, O_b and V atoms. PDOS (V) is fully symmetric in the valence and conduction bands and corresponds to the oxidation state V^{5+}. PDOS (O_t) and PDOS (O_b) are asymmetric at the top of the valence band. The detailed analysis of the spin polarization shows that the unpaired electron density is partially delocalized on the other oxygen atoms of the VO_4 unit as well [43]. It is possible to present the VO_4 active site as $(OO)^{-q}V^{5+}(O_bO_t)^{(-1+q)}$. As a result, the oxygen atoms of the O_t–V^{5+}–O_b surface species acquire properties typical for O^- radicals stabilized on the V^{5+} site. Recently similar VO_3/TiO_2 species were experimentally observed on (110) rutile surface and shown to be active in methanol dehydrogenation [39]. Based on the results of our simulations, it is very likely that the clusters observed in that study also had the properties of oxygen radicals.

Computational details

The calculations were performed using the QUANTUM ESPRESSO code [49] based on the spin-polarized density functional theory (DFT). Vanadium, titanium, oxygen, and carbon electron-core interactions were described by Vanderbilt Ultrasoft pseudopotentials [50] with exchange–correlation Perdew–Burke–Ernzerhof (PBE) functionals [51]. Wave functions of the valence electrons were expanded in plane waves with a kinetic energy cutoff 30 Ry. The charge density cutoff was 120 Ry. Brillouin zone sampling ($4 \times 2 \times 1$) was used. Electron structures of propane, isopropanol, isopropyl radical, and propene were calculated in the Γ point of the Brillouin zone. Figure 2 displays the optimized structures of these molecules.

The reaction pathways of the propane ODH were studied by the climbing image nudged elastic band method (CI-NEB) [52]. Eleven to 17 images (including 10–16 movable ones) were specified to locate the saddle points along the minimum energy path (MEP). This method allows one to determine the minimum energy paths and transition states with good precision. Optimization of the saddle point images was stopped at maximum force less than 0.05–0.06 eV/Å.

Results

Formation of propyl and isopropyl radicals

Several possible mechanisms regarding the activation of the C–H bond have been proposed [1–3]. The alkyl radical mechanism seems to be the most probable among

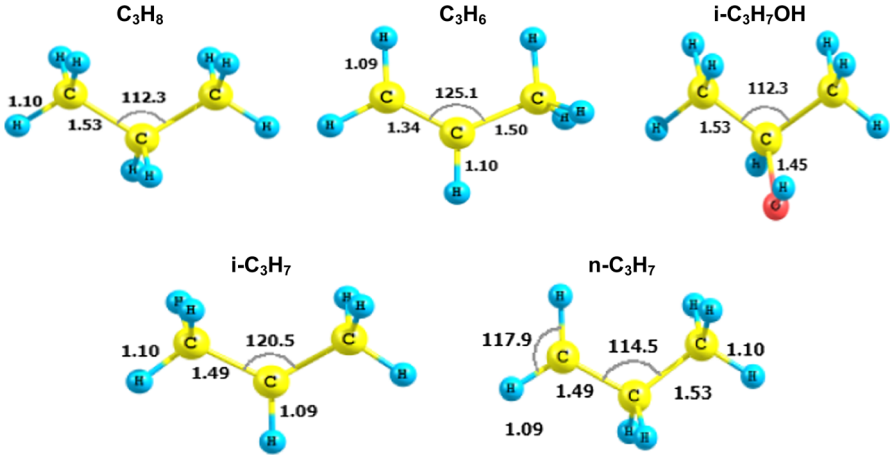

Fig. 2 Optimized structures of gas-phase propane, propene, isopropanol, propyl, and isopropyl radicals

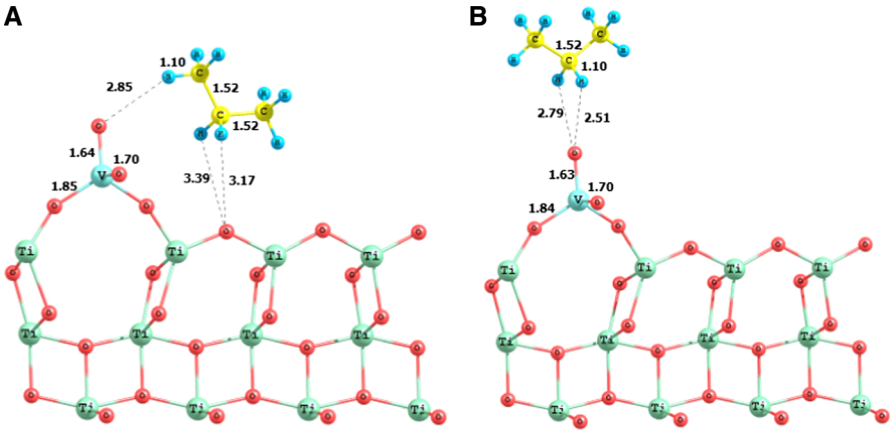

Fig. 3 The most stable structures of propane physical adsorption states over the VO_x/TiO_2 reconstructed model surface. These conformations start the activation of C_β–H and C_α–H bonds

them. Naturally, a radical mechanism can be started much easier from a radical active site.

The ODH reaction is preceded by physical adsorption of propane on the surface active site followed by activation of C–H bonds. The most stable structures are presented in Fig. 3. The estimation of adsorption energy ($\Delta E_{ads} < 0.01$ eV) suggests that physical adsorption of propane is nominal leading to the Eley–Rideal mechanism of the propane ODH reaction.

However, relative stability of the possible structural conformations can define the activation sequence of C_α–H and C_β–H bonds. The structural orientation shown in Fig. 3a initiates the hydrogen bond V–O_t···H–$CH_2CH_2CH_3$ followed by activation of the methyl C_β–H bond. In turn, the conformation shown in Fig. 3b initiates the

hydrogen bond V–O_t···H–$CH(CH_3)_2$ followed by activation of the methylene C_α–H bond. These processes lead to the formation of propyl and isopropyl radicals, respectively.

Figure 4 shows the reaction pathways for C_α–H and C_β–H bond activation followed by the hydrogen transfer to the terminal oxygen atom O_t of the active site $O_tV^{5+}O_b$. As a result, a surface hydroxyl group V–O_tH and a propyl or an isopropyl radical are formed:

$$C_3H_8 + [O_t - V^{5+}O_b] \rightarrow HO_t - V^{5+}O_b + (i,n) - [C_3H_7] \quad (1)$$

As shown in Fig. 4, the formation of *n*-C_3H_7 radical includes two steps. The first step corresponds to abstraction of a methyl hydrogen atom with the activation energy $E^* = 0.56$ eV. The second step corresponds to internal rotation along the CH_2–CH_2CH_3 bond with the activation energy $E^* = 0.26$ eV. No such additional barrier is observed for the formation of *i*-C_3H_7 radical. Both radicals are stabilized by weak physical adsorption ($\Delta E_{phys} \sim 0.01$ eV) on the surface site HO_t–$V^{5+}O_b$. According to our calculations and in accordance with several theoretical papers sited above, the activation of the C_α–H bond is both thermodynamically and kinetically more favorable than the activation of the C_β–H bond. Our estimations show that the formation of the *n*-C_3H_7 radical is kinetically less favorable by 0.10 eV than that of *i*-C_3H_7 ($E^* = 0.46$ eV).

Meanwhile, the sequence of the C–H bonds activation is controlled both by the geometric structure of the [VO_4] active site and by the electron distribution on the V–O bonds. Their subsequent transformations can follow different reaction pathways. We shall discuss two main possible pathways: *n*-C_3H_7 transformation to form propene and *i*-C_3H_7 conversion to form *i*-propanol. As it will be shown below, the first reaction pathway leads to the formation of adsorbed water, H_2O_t–

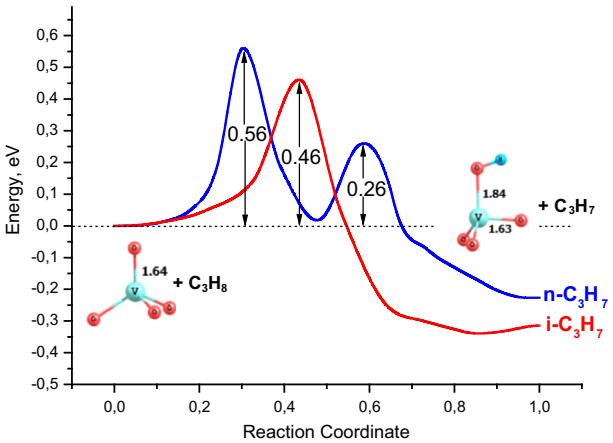

Fig. 4 Minimum energy pathways (MEP) for breaking of C_α–H and C_β–H bonds in propane resulting in the formation of *i*-C_3H_7 and *n*-C_3H_7 radicals, correspondingly. The *inset* structures in this and the following figures show only the [VO_4] structural unit. Full structural presentation of the reaction pathway is shown in the Supporting Information

$[V^{4+}]$–O_b. The second pathway leads to the formation of adsorbed propanol, *i*-$C_3H_7O_tH$–$[V^4]$–O_b. Both pathways result in the reduction of V^{5+} ion in the active site to V^{4+}.

Formation of propene

The propene formation pathway consists of two consecutive hydrogen abstraction steps. The first step includes the C_β–H bond activation in propane followed by the formation a surface hydroxyl group HO_t–$V^{5+}O_b$ and an *n*-C_3H_7 radical, as discussed above. The second step involves activation of the methylene C–H bond followed by hydrogen atom abstraction by the bridging oxygen atom O_b and one-electron reduction of the V^{5+} cation to V^{4+}. This reaction step is completed by the formation of the hydroxylated surface site and a propene molecule, which is eliminated to the gas phase.

$$HO_t - V^{5+}O_b + n\text{-}C_3H_7 \rightarrow HO_t - V^{4+} - O_bH + C_3H_6 \quad (2)$$

The corresponding reaction pathway is shown in Fig. 5.

As one can see from Figs. 4 and 5, both the primary and secondary C–H bonds are activated on a single isolated active site $[O_t$–V^{5+}–$O_b]$. Two active oxygen centers O_t and O_b linked with one vanadium ion V^{5+} demonstrate a synergic effect. At the first stage, the surface species HO_t–V^{5+}–O_b is formed. The oxygen atom O_b in this structure acquires the properties of a terminal vanadyl oxygen atom. Thus, the bi-functionality of the active site facilitates the hydrogen abstraction from propane to form propene.

Water formation

The reaction pathway of the hydrogen migration from one hydroxyl group to the other one to form adsorbed water is demonstrated in Fig. 6. The initial state

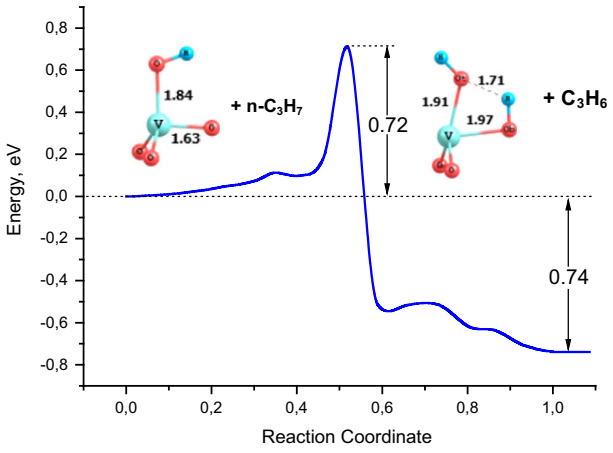

Fig. 5 MEP of the C_α–H bond activation of *n*-C_3H_7 radical leading to propene formation

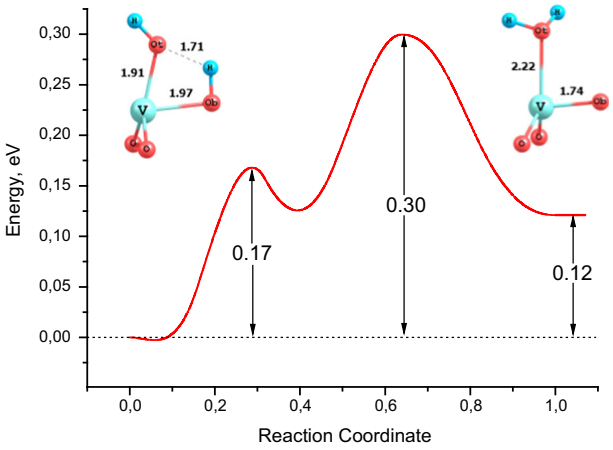

Fig. 6 MEP of the surface hydrogen transfer reaction HO–V^{4+}–OH → H_2O–V^{4+}–O to form water adsorbed on the reduced $V^{4+}O_x/TiO_2$ site

corresponds to the hydroxylated surface with two hydroxyl groups stabilized by one reduced V^{4+} site. Similar structural configuration starts the formation of the hydrogen bond V^{4+}–(H···O_t–H) followed by H-transfer to the oxygen atom of the hydroxyl group V–O_tH to form adsorbed water on the reduced site H_2O–V^{4+}. Our calculations give the activation energy $E^* = 0.30$ eV for this reaction.

Water desorption and subsequent reoxidation of the reduced V^{4+} site complete the catalytic cycle. We did not study the reaction pathways of these reactions. It is well known that reoxidation and water desorption are not the rate-determining steps of propane ODH. Although water desorption from the active site (3) is, as expected, an endothermal process, at elevated temperatures it is driven to completion by the entropy contribution.

Detailed mechanism of vanadium reoxidation by molecular oxygen (4) is beyond the scope of this study. In fact, it is never analyzed in detail in theoretical papers.

$$[V^{4+}] - H_2O \rightarrow [V^{4+}] + H_2O + \Delta H_{\text{des}}; \quad \Delta H_{\text{des}} = 0.56 \text{ eV} = 13.0 \text{ kcal/mol} \quad (3)$$

$$[V^{4+}] + 1/2O_2 \rightarrow V^{5+} - O^- + \Delta H_{\text{reox}}; \quad \Delta H_{\text{reox}} = -0.66 \text{ eV} = -15.2 \text{ kcal/mol} \quad (4)$$

As noted by us earlier [43], vanadium reoxidation over isolated vanadium sites is not as easy a process as it is commonly considered to be, even for the conventional mechanism involving the V^{3+}–V^{5+} pair. Obviously, it is somewhat more complicated for the V^{4+}–$V^{5+}O^-$ pair discussed in this manuscript. It may involve participation of O_2^- radical anions as it was suggested in our previous publication [43] or rupture of an oxygen molecule on two adjacent reduced metal ions. Residual organic groups or components of chemisorbed water present on the surface during

the catalytic reaction may also contribute to vanadia reoxidation. However, theoretical papers practically never address the reoxidation mechanism as it is well known that the oxide reoxidation is not the rate-determining reaction stage under optimal conditions [3, 4].

In fact, such reoxidation of reduced species to VO_3 species active in oxidative dehydrogenation was recently clearly demonstrated experimentally for a VO_x/TiO_2 catalyst [39]. In that publication, it was experimentally proven that such VO_3 radical species can indeed exist on the surface of VO_x/TiO_2 catalysts and are the only species active in oxidative dehydrogenation of methanol [39]. Also, reoxidation of V^{4+} ions by molecular oxygen at a low temperature to form $V^{5+}O^-$ radicals experimentally observed by EPR is well documented for VO_x/SiO_2 [38]. Thus, there is no doubt that reoxidation of most if not all V^{4+} ions to $V^{5+}O^-$ by molecular oxygen is experimentally possible, although additional studies are required to understand its mechanism in detail.

Selective oxidation of propane to isopropanol

The initial stages of propane selective oxidation to isopropanol and oxidative dehydrogenation to propene are similar. Figure 7 shows the reaction pathway for the formation of isopropyl radical followed by incorporation of i-C_3H_7 radical into the V^{5+}–O_tH bond resulting in the formation of isopropanol adsorbed on the reduced V^{4+} site (*5*).

$$V^{5+} - O^- + C_3H_8 \rightarrow V^{5+} - OH + [i\text{-}C_3H_7] \rightarrow V^{4+} - [i\text{-}C_3H_7OH] \qquad (5)$$

Isopropanol desorption (6) and subsequent reoxidation of the active site (4) complete the catalytic cycle for selective propane oxidation to isopropanol. At elevated temperatures used for the catalytic reaction, isopropanol should be able to desorb from the reduced surface site. However, it is likely to undergo subsequent dehydration to form propene. Still, isopropanol remaining on the surface may be subjected to further oxidation and initiate the deep oxidation pathway.

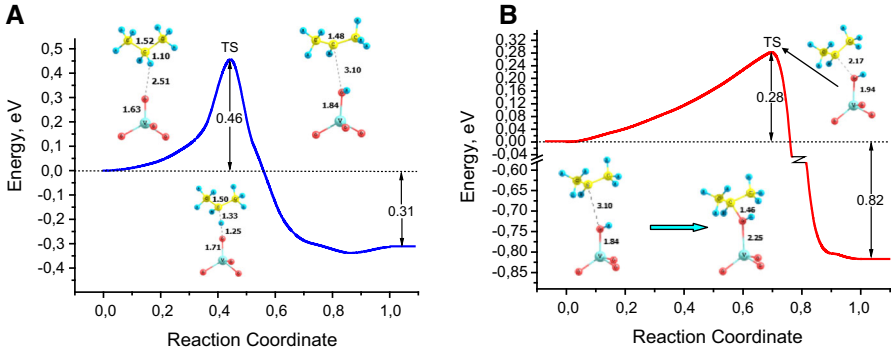

Fig. 7 Reaction pathways for activation of the C_α–H bond of the isopropyl radical (**a**) resulting in the formation of adsorbed isopropanol (**b**)

$$[V^{4+}] - [i\text{-}C_3H_7OH] \rightarrow i\text{-}C_3H_7OH + [V^{4+}]; E_{des}(C_3H_7OH) = 0.25 \text{ eV} = 5.8 \text{ kcal/mol} \quad (6)$$

Discussion

Recently, Alexopoulos et al. [19] carried out detailed analysis of oxidative dehydrogenation processes and reaction pathways over V_2O_5 and V_2O_5/TiO_2 by periodical DFT. They used a model of the V_2O_5/TiO_2 catalyst where surface species VO_x were constructed over a regular (not reconstructed) anatase-TiO_2 (001) surface. The authors concluded that selective oxidation of propane to propanol and its oxidative dehydrogenation to propene proceed according to a Mars–van-Krevelen redox mechanism that involves two-electron reduction $V^{5+} \rightarrow V^{3+}$.

The main difference of the results reported in this manuscript is that the first, supposedly the most difficult, hydrogen abstraction step becomes quite easy when we use a surface oxygen radical as the surface active site. In our mechanism V^{5+} is reduced only to V^{4+}. The second electron of the overall two-electron oxidation process comes from the oxygen radical. The formation of V^{4+} ions during ODH and other selective oxidation reactions on vanadia catalysts has been observed in numerous experimental studies. For instance, transient kinetic modeling of the oxidative dehydrogenation of propane over V/TiO_2 catalyst shows that the reduced states of the catalyst consist of a mixture of V^{4+} and V^{3+} with the former in large excess [53].

The radical reaction pathway started on surface oxygen radicals is frequently believed to lead to deep oxidation products. However, this assumption seems to be seriously questioned by the high selectivity of such species in Fe-ZSM-5 catalysts and related arguments by Panov et al. [54].

Because of its higher activity, propene will readily participate in reaction with any site where propane is converted. The keys to high selectivity here are: (1) lack of propene reaction with the reduced site where it is formed; and (2) lack of propene reaction with abundant adjacent sites. To avoid undesired deep oxidation of the primary product, it is necessary to have few active sites next to the original adsorption site, where the adsorbed paraffin can undergo deeper oxidation. If there are few very active sites reacting both with propane and propene, while most of the surface species are inactive with respect to either reagent, than higher activity of propene will no longer be the key. In this case the selectivity will mostly depend on conversion, i.e. propane/propene ratio on the surface. Short contact times will help to increase selectivity. The same ideas were suggested in conclusion of a recent detailed review by Carrero et al. [4].

We believe that our oxygen radical model of the active site is ideally suited to this concept. Both of the mentioned key conditions are realized in the suggested mechanism. The propene adsorption energy on the formed reduced surface site is very low. This should allow for its quick desorption from the surface. Further propene oxidation requires its readsorption on a different active site where it can be oxidized. It is exceptionally important that the concentration of oxygen radical sites on the surface is low. Relative isolation of the active vanadium species containing

the radical form of oxygen should make selective oxidation the main reaction pathway. No active oxygen atoms remain on the active site after the propene formation. Oxygen movement from the bulk to the reduced surface site is also very limited for supported vanadia catalysts. Thus, the released propene, which is more susceptible to oxidation than propane, should not be immediately involved in further oxidation, unless it reaches another radical site after migrating over the surface.

The suggested active site seems to have correct functionality for the oxidative dehydrogenation reaction. The first hydrogen atom is abstracted by the surface oxygen radical with low activation energy. The diamagnetic vanadium species formed at this step has another relatively active vanadyl oxygen atom. It can readily accept another hydrogen atom abstracted from an organic radical formed at the first step. No more active oxygen atoms that could start further oxidation remain on the active site after the second step. All these factors combined suggest that propene oxidative dehydrogenation on the oxygen radical species on the surface of VO_x/TiO_2 catalyst simulated in this study should be a selective process.

On the contrary, if conventional vanadyl groups commonly believed to be the active sites were the places where this reaction takes place, the released propene molecule would be involved in further oxidation processes immediately upon migrating to any adjacent V^{5+} site present in high concentration on the surface. This would make the desired high selectivity practically unachievable. So, we believe that oxygen radical species are the most likely candidates to the role of very active species present in low concentration among many less active ones, which was recently suggested to be the key factor for a selective oxidative dehydrogenation catalyst [4].

The complete pathway for propane ODH in a uniform energy scale is presented in Fig. 8. The first hydrogen abstraction reaction appears to be the rate-determining step of the overall ODH process. Our computations prove that the surface oxygen

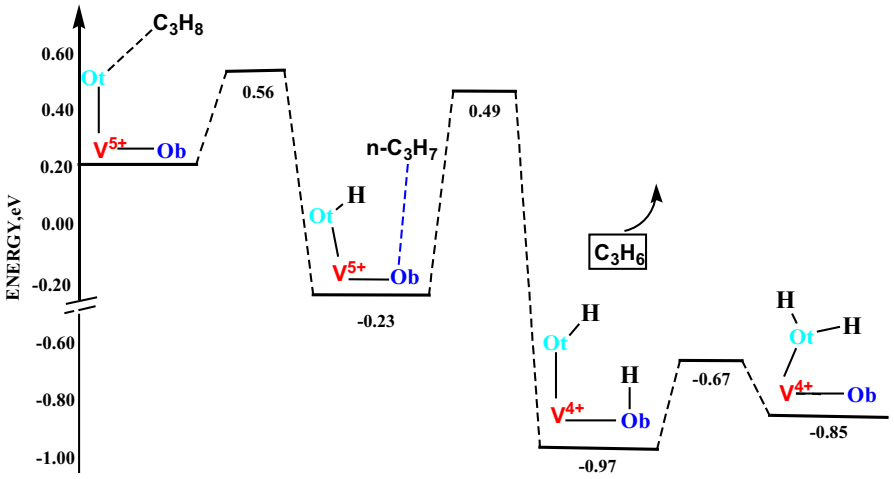

Fig. 8 Energy diagram of propane conversion to propene on the [O_t–V^{5+}–O_b] active site of the (1 × 4)-reconstructed VO_x/TiO_2 surface

radical species forming on the supported vanadium oxide catalyst VO_x/TiO_2 are very reactive and can abstract hydrogen atoms from propane with low activation energy $E^* = 0.56$ eV. In our calculation the energetic barrier of the second stage was slightly lower. Still both values are very close. So, their relative importance may depend on the used model and DFT functional.

This value is close to many reported experimental results discussed in Introduction. The theoretical data reported in this paper prove that the experimental activation energies for propane ODH over VO_x/TiO_2 catalysts can be readily reproduced if oxygen radicals are considered to be the active sites where propane molecules are activated.

All O^- radicals observed by EPR proved to be very reactive. In particular, it was shown that atomic oxygen radicals O^- on VO_x/SiO_2 reacted with H_2, CO, C_2H_4, or C_6H_6 at very low temperatures [54, 55]. It was suggested that O^- radicals were responsible for oxidative dimerization of methane at elevated temperatures over-promoted MgO catalysts [34]. Homolytic splitting of methane molecules with the formation of methyl radicals appeared to be clear evidence for participation of O^- radicals in this reaction. Apparently, the elevated temperatures were required for generation of the radicals in sufficient concentrations as their reaction with methane was reported to take place at temperatures below ambient.

For propane ODH over VO_x/TiO_2 catalysts, we also believe that high temperatures are required for generation of the active radical species in sufficient concentrations. For the reaction to take place above 450 °C with relatively low experimental activation energy, the concentration of the active sites should be low. Therefore, oxygen radicals generated in low concentrations at elevated temperatures are quite capable of acting as such active sites. The results obtained in this paper demonstrate that the energy barrier required for propane dehydrogenation over oxygen radicals formed on the surface of VO_x/TiO_2 catalysts is in a good agreement with the experimental activation energies.

Earlier we reported that reaction of the same oxygen radicals on the surface of VO_x/TiO_2 catalysts with hydrogen is slightly endothermic with reaction enthalpy +13 kcal/mol [43]. The results obtained in this study demonstrate that V^{5+}–O^- radicals on the TiO_2 surface should be able to react with propane at relatively low temperatures with low activation energy. One should expect these O^- radicals to be capable of reacting with various saturated hydrocarbons that are known to be oxidized on the surface of VO_x/TiO_2 catalysts as well. On the contrary, participation of neutral V^{5+} species in many such reactions is strongly energetically unfavorable.

Detailed structure of oxygen radicals on the surface of vanadia supported on oxide supports other than anatase titania is certainly somewhat different than on the studied surface. The analysis of propane ODH mechanism over such catalysts is beyond the scope of this study. However, we do not expect the calculated intrinsic activation energies of the ODH reaction stages on radical active sites to depend significantly on the type of the used support. The differences in the apparent activation energies over vanadia catalysts deposited on different oxide supports are, most likely, related to the thermodynamics of the oxygen radical generation that must depend on the used support. In fact, this may be the key to understanding the experimentally observed dependence of the catalytic activity on the reducibility of

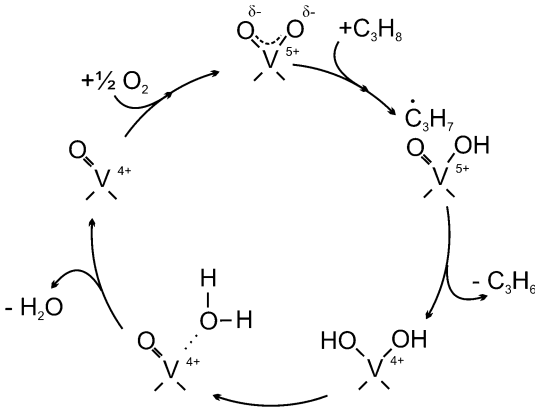

Fig. 9 Catalytic cycle for propane ODH over V^{5+}–O^{-} radical cite

the support [4]. A comprehensive theoretical analysis of this stage and the effect of the support on the radical generation is in our future plans.

The catalytic cycle for propane ODH on the studied radical active sites is shown in Fig. 9. The first stage is hydrogen atom abstraction by surface oxygen radical to form a propyl radical and a saturated V^{5+} site. The second stage is the reaction of the vanadyl oxygen with the propyl radical to form propene released into the gas phase and hydroxylated reduced vanadium species V^{4+}. The third stage is hydrogen atom migration from one hydroxyl group of this reduced form to the other one the form adsorbed water. Water desorption and reoxidation of the surface site with an oxygen atom regenerate the active site.

Overall, the results obtained in this study call for more detailed theoretical and experimental studies of the possible role of oxygen radicals in various selective oxidation processes. In our opinion, such surface oxygen radicals should be seriously considered in the studies analyzing the catalytically active sites of oxidation catalysis and mechanisms of reactions taking place on them. We hope that the reported results will stimulate interest of researchers to experimental and theoretical studies of surface oxygen radicals as active sites of different selective oxidation reactions. Various experimental methods should be attempted for detection and quantification of the surface oxygen radicals, which seem to be not observed by EPR directly.

Conclusions

The results presented in this paper demonstrate that oxidative dehydrogenation of propane can proceed with low activation energies over oxygen radicals stabilized on the surface of VO_x/TiO_2 catalysts. Earlier possible existence of such sites was suggested by us based on the simulation of oxygen isotopic exchange on VO_x/TiO_2 [43]. Participation of V^{5+}–O^{-} oxygen radicals as the active sites of propane ODH substantially lowers the energetic barrier of the first hydrogen abstraction step, which is usually considered to be the rate-determining step of this reaction. The

activation energy obtained for this step in our study is as low as 0.56 eV. This value is in excellent agreement with low values of apparent activation energy reported for this reaction on VO_x/TiO_2 catalysts. Meanwhile, the fact that this reaction with low activation energy takes place at 450 °C or higher temperatures suggests that the concentration of active is relatively low. Thus, it is unlikely to take place on the abundant surface vanadium species.

The obtained data indicate that oxygen radical species can be the active sites in this and other heterogeneous selective oxidation reactions. Further studies of reaction mechanisms with the emphasis on possible participation of such radicals in various catalytic reactions seem to be very important. Also, it is crucial to develop experimental methods for detection and quantitative investigation of such species, which are very elusive due their high activity.

Acknowledgments This work was supported by the Russian Foundation for Basic Research (Grants 14-03-01110 and 15-03-08070).

References

1. H.H. Kung, Adv. Catal. **40**, 1 (1994)
2. E.A. Mamedov, V.C. Corberan, Appl. Catal. A-Gen. **127**, 1 (1995)
3. R. Grabowski, Catal. Rev.-Sci. Eng. **48**, 199 (2006)
4. C. Carrero, R. Schloegl, I. Wachs, R. Schomaecker, ACS Catal. **4**, 3357 (2014)
5. V.V. Chesnokov, A.F. Bedilo, D.S. Heroux, I.V. Mishakov, K.J. Klabunde, J. Catal. **218**, 438 (2003)
6. I.V. Mishakov, E.V. Ilyina, A.F. Bedilo, A.A. Vedyagin, React. Kinet. Catal. Lett. **97**, 355 (2009)
7. E.V. Ilyina, I.V. Mishakov, A.A. Vedyagin, S.V. Cherepanova, A.N. Nadeev, A.F. Bedilo, K.J. Klabunde, Microporous Mesoporous Mater. **160**, 32 (2012)
8. B. Beck, M. Harth, N.G. Hamilton, C. Carrero, J.J. Uhlrich, A. Trunschke, S. Shaikhutdinov, H. Schubert, H.J. Freund, R. Schlogl, J. Sauer, R. Schomacker, J. Catal. **296**, 120 (2012)
9. J.K. Lee, U.G. Hong, Y. Yoo, Y.J. Cho, J. Lee, H. Chang, I.K. Song, J. Nanosci. Nanotechnol. **13**, 8110 (2013)
10. E.V. Ilyina, I.V. Mishakov, A.A. Vedyagin, A.F. Bedilo, K.J. Klabunde, Microporous Mesoporous Mater. **175**, 76 (2013)
11. A.F. Bedilo, E.I. Shuvarakova, A.M. Volodin, E.V. Ilyina, I.V. Mishakov, A.A. Vedyagin, V.V. Chesnokov, D.S. Heroux, K.J. Klabunde, J. Phys. Chem. C **118**, 13715 (2014)
12. C.A. Carrero, C.J. Keturakis, A. Orrego, R. Schomacker, I.E. Wachs, Dalton Trans. **42**, 12644 (2013)
13. I. Rossetti, G.F. Mancini, P. Ghigna, M. Scavini, M. Piumetti, B. Bonelli, F. Cavani, A. Comite, J. Phys. Chem. C **116**, 22386 (2012)
14. N.U. Zhanpeisov, S. Higashimoto, M. Anpo, Int. J. Quantum Chem. **84**, 677 (2001)
15. N.U. Zhanpeisov, Res. Chem. Intermed. **30**, 133 (2004)
16. H. Fu, Z.P. Liu, Z.H. Li, W.N. Wang, K.N. Fan, J. Am. Chem. Soc. **128**, 11114 (2006)
17. X. Rozanska, E.V. Kondratenko, J. Sauer, J. Catal. **256**, 84 (2008)
18. N.N. Ha, N.D. Huyen, L.M. Cam, Appl. Catal. A-Gen. **407**, 106 (2011)
19. K. Alexopoulos, M.F. Reyniers, G.B. Marin, J. Catal. **289**, 127 (2012)
20. Y.J. Du, Z.H. Li, K.N. Fan, J. Mol. Catal. A-Chem. **379**, 122 (2013)
21. L. Cheng, G.A. Ferguson, S.A. Zygmunt, L.A. Curtiss, J. Catal. **302**, 31 (2013)
22. I. Muylaert, P. Van Der Voort, Phys. Chem. Chem. Phys. **11**, 2826 (2009)
23. A. Dinse, B. Frank, C. Hess, D. Habel, R. Schomacker, J. Mol. Catal. A-Chem. **289**, 28 (2008)
24. D. Shee, T. Rao, V, G. Deo. Catal. Today **118**, 288 (2006)
25. R.P. Singh, M.A. Banares, G. Deo, J. Catal. **233**, 388 (2005)
26. D.A. Medvedev, A.A. Rybinskaya, R.M. Kenzhin, A.M. Volodin, A.F. Bedilo, Phys. Chem. Chem. Phys. **14**, 2587 (2012)
27. A.F. Bedilo, E.I. Shuvarakova, A.A. Rybinskaya, D.A. Medvedev, J. Phys. Chem. C **118**, 15779 (2014)

28. A.F. Bedilo, A.M. Volodin, Kinet. Catal. **50**, 314 (2009)
29. R.A. Zotov, V.V. Molchanov, A.M. Volodin, A.F. Bedilo, J. Catal. **278**, 71 (2011)
30. R.M. Richards, A.M. Volodin, A.F. Bedilo, K.J. Klabunde, Phys. Chem. Chem. Phys. **5**, 4299 (2003)
31. S.E. Malykhin, A.M. Volodin, A.F. Bedilo, G.M. Zhidomirov, J. Phys. Chem. C **113**, 10350 (2009)
32. M. Che, A.J. Tench, Adv. Catal. **31**, 77 (1982)
33. A.M. Volodin, Catal. Today **58**, 103 (2000)
34. C.H. Lin, T. Ito, J.X. Wang, J.H. Lunsford, J. Am. Chem. Soc. **109**, 4808 (1987)
35. V.A. Shvets, V.B. Kazansky, J. Catal. **25**, 123 (1972)
36. H. Launay, S. Loridant, D.L. Nguyen, A.M. Volodin, J.L. Dubois, J.M.M. Millet, Catal. Today **128**, 176 (2007)
37. E.V. Kondratenko, A. Bruckner, J. Catal. **274**, 111 (2010)
38. A.M. Volodin, V.A. Bolshov, Kinet. Catal. **34**, 142 (1993)
39. S.P. Price, X. Tong, C. Ridge, H.L. Neilson, J.W. Buffon, J. Robins, H. Metiu, M.T. Bowers, S.K. Buratto, J. Phys. Chem. A **118**, 8309 (2014)
40. V.I. Avdeev, V.N. Parmon, J. Phys. Chem. C **113**, 2873 (2009)
41. V.I. Avdeev, V.M. Tapilin, J. Phys. Chem. C **114**, 3609 (2010)
42. V.I. Avdeev, A.F. Bedilo, J. Phys. Chem. C **117**, 2879 (2013)
43. V.I. Avdeev, A.F. Bedilo, J. Phys. Chem. C **117**, 14701 (2013)
44. G.S. Herman, M.R. Sievers, Y. Gao, Phys. Rev. Lett. **84**, 3354 (2000)
45. M. Lazzeri, A. Selloni, Phys. Rev. Lett. **87**, 266105 (2001)
46. S.T. Choo, Y.G. Lee, I.S. Nam, S.W. Ham, J.B. Lee, Appl. Catal. A-Gen. **200**, 177 (2000)
47. O.B. Lapina, A.A. Shubin, A.V. Nosov, E. Bosch, J. Spengler, H. Knozinger, J. Phys. Chem. B **103**, 7599 (1999)
48. S. Albonetti, F. Cavani, F. Trifiro, Catal. Rev.-Sci. Eng. **38**, 413 (1996)
49. P. Giannozzi, S. Baroni, N. Bonini, M. Calandra, R. Car, C. Cavazzoni, D. Ceresoli, G.L. Chiarotti, M. Cococcioni, I. Dabo, A. Dal Corso, S. de Gironcoli, S. Fabris, G. Fratesi, R. Gebauer, U. Gerstmann, C. Gougoussis, A. Kokalj, M. Lazzeri, L. Martin-Samos, N. Marzari, F. Mauri, R. Mazzarello, S. Paolini, A. Pasquarello, L. Paulatto, C. Sbraccia, S. Scandolo, G. Sclauzero, A.P. Seitsonen, A. Smogunov, P. Umari, R.M. Wentzcovitch, J. Phys.-Condens. Matter **21**, 395502 (2009)
50. D. Vanderbilt, Phys. Rev. B **41**, 7892–7895 (1990)
51. J.P. Perdew, K. Burke, M. Ernzerhof, Phys. Rev. Lett. **77**, 3865 (1996)
52. G. Henkelman, B.P. Uberuaga, H. Jonsson, J. Chem. Phys. **113**, 9901 (2000)
53. V. Balcaen, I. Sack, M. Olea, G. Marin, Appl. Catal. A-Gen. **371**, 31 (2009)
54. G.I. Panov, K.A. Dubkov, E.V. Starokon, Catal. Today **117**, 148 (2006)
55. S.A. Surin, A.D. Shuklov, B.N. Shelimov, V.B. Kazanskii, Kinet. Katal. **19**, 435 (1978)